ChemComm

Cite this: *Chem. Commun.*, 2012, **48**, 1781–1783

www.rsc.org/chemcomm

**COMMUNICATION**

# Multiple homogeneous immunoassays based on a quantum dots–gold nanorods FRET nanoplatform†

**Qinghui Zeng,[a] Youlin Zhang,[a] Xiaomin Liu,[a] Langping Tu,[a] Xianggui Kong*[a] and Hong Zhang*[b]**

***Received 9th October 2011, Accepted 7th December 2011***
**DOI: 10.1039/c2cc16271g**



**Multi-sized quantum dots (QDs) donors and tailor-made gold nanorods (GNRs) are employed to form a FRET nanoplatform for homogeneous immunoassays developed for analysis of multiple virus antigens. The single GNRs/multiple QDs nanocomposite based nanosensor offers a simple and sensitive approach for multiple analytes detection in a homogeneous format.**

Homogeneous immunoassays (HIA) are becoming more and more attractive for modern medical diagnosis and analyte detection because they are superior to heterogeneous immunoassays in sample and reagent consumption, analysis time, portability and disposability.[1] Most importantly, there is no need for separation and purification of the labelled biological molecules, which often lead to a drop in the biological specificity of the labelled biomolecules resulting in the decrease of the sensitivity of the analyte detection.[2] An important sort of HIA being more and more popular in bioanalytical and biosensing applications relies on fluorescence resonance energy transfer (FRET) by constructing a donor–acceptor (DA) system in aqueous solution.[3] With the enhanced security and health concern worldwide, highly sensitive and selective sensors capable of simultaneous detection of multiple analytes become one of the focuses in the scientific community. The requirement of rapid assay, simple procedure, low sample and reagent consumption makes multiple assays preferable to single-target assays.[4]

Obviously, the key to improve the detection sensitivity of FRET-based HIA is to enhance the FRET efficiency. General and feasible approaches include increasing the spectral overlap between donor's emission and acceptor's absorption, and/or increasing the extinction coefficient of the acceptor.[5,6] Traditional FRET-based HIA usually use fluorescent dyes as the donors or acceptors. Disadvantages of these dyes, *e.g.*, feasible photobleaching, weak photostability, wide emission spectra and narrow absorption bands restrain their applications in multiple HIA. Through overcoming these disadvantages, quantum dots (QDs) and quantum rods have in recent years merged in this field as better donor candidates.[3,7–10] QDs are thus extremely suitable for the fluorescence variation induced multiplex labeling and multiple immunoassays.

Gold nanorods (GNRs) display two separate localized surface plasmon resonances in the visible/near-IR spectral range, due to transverse and longitudinal oscillations of conduction electrons. GNRs should thus be better multiple acceptor candidates because their scattering and absorption bands can be tuned by adjusting the aspect ratio of the nanorods and their *high extinction coefficient*.[6,8,11] However, the most popular GNRs' plasmon resonance absorption is located in the near-infrared region, segregating far away from the emission window of the popular CdSe or CdTe QDs which often localize in the visible region; in addition, the double plasmon absorption peaks are often not comparative. In most cases, the optical density and extinction coefficient of the long-wavelength peak are greatly higher than those of the short-wavelength peak, which adversely impact the synchronously multiple immunoassays based on FRET between a single GNR and multiple QDs.

To circumvent this restriction, we have prepared the *low aspect ratio* GNRs with two comparative plasmon absorption peaks *via* the approach of self-assembly growth of the generally high aspect ratio GNRs (Scheme S1, ESI†). QDs' emission and GNRs' plasmon absorption were size-tuned to guarantee an efficient FRET yield by optimizing the overlap of QDs' emission and the two absorption bands of the GNRs.[6,12] Furthermore we extended our sensor design beyond the previous prototype[6,11] and demonstrate the QDs–GNRs based FRET nanosensor for multiple detections of Hepatitis B surface antigen (HBsAg) and Hepatitis B e antigen (HBeAg). As shown in Scheme 1, HBsAb1 and HBeAb1, specifically immobilized on the surfaces of GNRs, acted as FRET acceptors. On the other hand, HBsAb2 and HBeAb2, specifically immobilized on the surface of green CdTe/CdS core/shell QDs (GQDs, $\lambda_{em}$ = 521 nm) and red CdTe/CdS core/shell QDs (RQDs, $\lambda_{em}$ = 629 nm), respectively, played a role of FRET donors. Addition of target HBsAg and HBeAg to the HIA system caused the immunoreactions induced sandwich construction between bull serum albumin (BSA) blocked QDs–Ab and GNRs–Ab bio-conjugates and resulted in concentration-dependent FRET processes. The photoluminescence

[a] *State Key Laboratory of Luminescence and Applications, Changchun Institute of Optics, Fine Mechanics and Physics, Chinese Academy of Sciences, 3888 Eastern South Lake Road, Changchun 130033, China. E-mail: xgkong14@ciomp.ac.cn; Tel: +86-431-86176313*
[b] *Van't Hoff Institute for Molecular Sciences, University of Amsterdam, Science Park 904, 1098 XH Amsterdam, The Netherlands. E-mail: h.zhang@ uva.nl; Tel: +31-20-5256976*

† Electronic supplementary information (ESI) available: Experimental and instrumental details, Scheme S1–S3 and Fig. S1–S6. See DOI: 10.1039/c2cc16271g

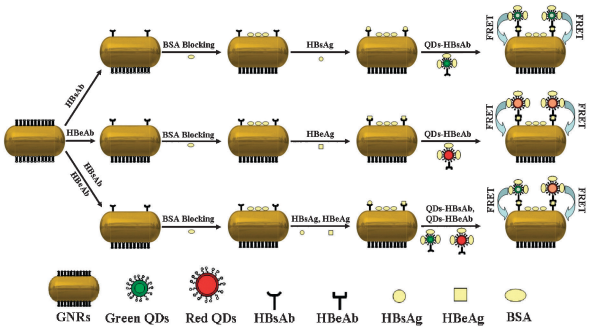


**Scheme 1** The schematic single and multiple immune detection procedure of HBsAg, HBeAg and the mixture of HBsAg and HBeAg based on FRET from GQDs, RQDs and the mixture of GQDs and RQDs to GNRs.

(PL) of both GQDs and RQDs were quenched by the GNRs immediately. The HBsAg and HBeAg were tested synchronously against the HIA to determine the detection sensitivity, specificity and detection range. To the best of our knowledge, this contribution describes the first instance of employing multi-sized QDs donors and single GNRs acceptors to form a FRET nanoplatform for multiple homogeneous immune assays of virus antigens. The GNRs–QDs based HIA is a simple "mix and detection" nanoplatform with extremely low sample consumption, high sensitivity, and short analysis time and has the potential for rapid point-of-care testing, high-throughput screening, and clinical diagnostics.

Synthesis of the gold nanorods was a seed-mediated growth procedure, in which Au salts were reduced initially with a strong reducing agent to produce seed particles. Briefly, the high aspect ratio gold nanorods with plasmon absorption peaks at 509 and 776 nm were firstly prepared *via* using hexadecyltrimethylammonium bromide (CTAB) as surface ligand.[13] Scheme S1 (ESI†) illustrates schematically the growth process of the high aspect ratio and low aspect ratio GNRs. The low aspect ratio nanorods were prepared by the self-assembling approach of the original nanorods of the high aspect ratio (see ESI† for experimental details). As shown in Fig. 1, the aspect ratio of GNRs gradually evolved from 3.5 to 2.9, 2.3, and ultimately 1.9 with different growth times. The evolution could be monitored well from either the FE-SEM results or the absorption spectra. The ratio of the optical density between the transverse and longitudinal plasmon bands was accordingly evolved from 1 : 7.0, to 1 : 4.8, 1 : 2.4 and 1 : 1.6. In our case, the low aspect ratio GNRs (aspect ratio = 1.9) were selected to be the acceptor for the HIA because the optical density and extinction coefficient of the short-wavelength peak are greatly close to the long-wavelength peak.

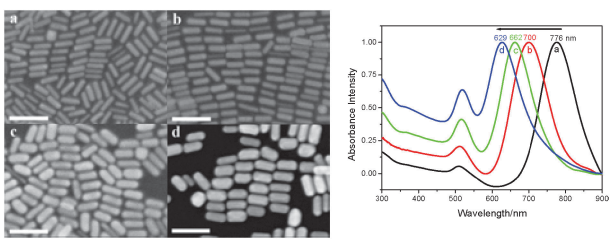


**Fig. 1** FE-SEM images of the GNRs with different aspect ratio prepared self-assemblies and the relative normalized plasmon absorption spectra of the samples. The scale bar is 100 nm.

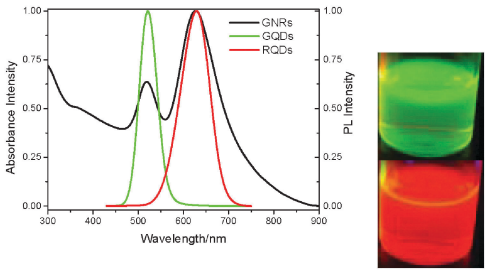


**Fig. 2** Normalized absorption spectrum of GNRs (black line) and PL spectra of green and red QDs. The photos at the right side are taken from the respective GQDs and RQDs.

Since the tailored low aspect ratio GNRs have comparative plasmon absorption peaks at 520 and 629 nm, we selected green QDs-521 and red QDs-629 to confirm that the emissions of the QDs could match well with the absorption of the GNRs (shown in Fig. 2). The QDs were capped with negatively charged 3-mercaptopropionic acid, and the GNRs were capped with positively charged CTAB molecules. Thus the QDs and GNRs could readily combine with each other through electrostatic interactions. Consequently, the photoluminescence of GQDs and RQDs would be efficiently quenched by the GNRs due to the nonradiative FRET process. As shown in Fig. S1 (ESI†), when the volume of GNRs added into the QDs solution was increased from 5 to 10, 20, 40 μL, and upwards, the PL of both single color QDs and equally proportional mixture of double color QDs quenched well and the quenching tended to be saturated after a constant volume (~80 μL) of GNRs. From the PL spectra shown in Fig. S1a and b (ESI†), the FRET efficiency could achieve 87.6% for GQDs and 91.1% for RQDs as the volume of GNRs reaches the saturated value. Such high FRET efficiencies were attributed to a combination of factors, such as considering the characteristics of the present design and the rule of FRET efficiency.[7] Because the PL quenching of QDs is GNRs' dosage relative, we could carry out the HIA according to the fluorescent quenching of QDs when the bright and robust QDs (shown in Fig. 2) were coupled with biomolecules to function as the detection indicator.

As far as virus is concerned, Hepatitis B virus was chosen to perform HIA based on the QDs–GNRs FRET nanoplatform. The schematic HIA procedure of HBsAg or HBeAg based on FRET from QDs to GNRs is given in Scheme 1. To start the test, the GNRs–Ab1 and QDs–Ab2 were first mixed in a homogeneous solution. When the analyte-Ag molecules were added into the homogeneous solution, the GNRs–Ab1/Ag/QDs–Ab2 sandwich structure should be formed after the immunoreactions and the FRET from QDs to GNRs would then occur. As shown in the inset of Fig. 3a and Fig. S3 (ESI†), the emission quenching displayed an evolving FRET process in proportion to the increase in the amount of detected antigens. The detection curves of the antigens were acquired as the difference between PL intensities of the control value of QDs–Ab without Ag and GNRs–Ab1/Ag/QDs–Ab2 sandwich structures. Fig. 3a and Fig. S3 (ESI†) illustrate the PL spectra of multiple HIA system and single HIA system with different concentrations of antigens. It should be noted that the signal increased monotonically with the increase of the concentration

 

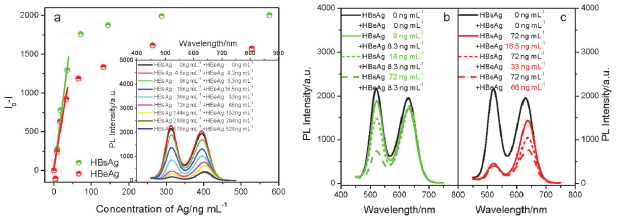


**Fig. 3** FRET-based multiple detection of antigens (a). The relationship between the subtracted PL intensity ($I_0 - I$) of the mixture of GQDs–HBsAb2 and RQDs–HBeAb2 in the presence of GNRs–Ab1 and the detected mixture of HBsAg and HBeAg with different concentrations. Inset is the relative PL spectra variation of the mixture of GQDs and RQDs. The variation of the PL spectra based on the multiple detection when the concentrations of the detected HBeAg (b) and HBsAg (c) are kept constant.

of HBsAg (or HBeAg) until 288 (or 264) ng mL$^{-1}$. Hereby, the detection range of HBsAg (or HBeAg) can achieve 288 (or 264) ng mL$^{-1}$ for multiple immunoassays. The linear calibration curve could be obtained as $Y = 7.195 + 36.83X$ ($9 \leq X \leq 36$ ng mL$^{-1}$, $R = 0.991$) and $Y = 38.756 + 28.39X$ ($8.3 \leq X \leq 33$ ng mL$^{-1}$, $R = 0.979$) for multiple HBsAg and HBeAg detection by using GQDs and RQDs common compounds as donors. The limit of detection (LOD) can be defined as the lowest concentration of the detected sample that gives a positive value of the PL intensity difference between the control (without antigen) and the detected sample (with antigen).[14,15] It can be clearly seen from Fig. 3 and Fig. S3 (ESI†) that the subtracted PL intensity was still discernable to be positive even when the concentrations of HBsAg and HBeAg were as low as about 9.0 ng mL$^{-1}$ and 8.3 ng mL$^{-1}$ for the multiple HIA. However, similar to the results from Fig. S1d (ESI†), it was also observed that after multiple HIA the detection curves of the HBsAg (using GQDs) and HBeAg (using RQDs) were higher and lower than the curves of the single detection as soon as the concentration of the target antigens surpassed 36 and 33 ng mL$^{-1}$, respectively (Fig. S4, ESI†). These observations might well be an indication of the unavoidable FRET process from GQDs to RQDs themselves.[16] As a result, we can practice the exceedingly accurate multiple detection under a relative low concentration condition and highly sensitive detection requirement (*e.g.*, $\leq$36 ng mL$^{-1}$ for HBsAg and $\leq$33 ng mL$^{-1}$ for HBeAg).

Because the structure and topography properties of HBsAg and HBeAg are very similar to each other, it is thus necessary to detect the HBsAg (or HBeAg) when the concentration of HBeAg (or HBsAg) was kept constant to confirm the specificity of the multiple HIA. As shown in Fig. 3b and c, when the detected HBeAg (Fig. 3b) and HBsAg (Fig. 3c) were kept constant at 8.3 and 72 ng mL$^{-1}$, respectively, multiple detections could still be realized. For example, in the case that concentration of HBeAg in the homogeneous format was constant the green PL decreased in relation to the increase in the detected HBsAg. Similar result was obtained for red PL when HBsAg was constant to detect the HBeAg. At the same time, the PL intensity of RQDs for HBsAg detection and that of GQDs for HBeAg detection showed negligible change, demonstrating a highly specific detection.

In order to eliminate the possibility of the re-absorption of GNRs on the QDs' emission, we also measured the PL spectra when the BSA blocked QDs–Ab and GNRs–Ab bio-conjugates were mixed. Without the electrostatic adsorption and/or sandwich construction, the QDs and GNRs in this system could not connect with each other. FRET is accordingly impossible. As shown in Fig. S5 (ESI†), the PL spectra of QDs remained almost constant with the increase of the concentration of BSA blocked GNRs–Ab solution. This result confirmed that contributions from non-resonant or non-specific interactions were essentially negligible. To further demonstrate the high specificity of the FRET based HIA, we also performed some non-specific detection (see details in ESI†). It can be concluded that our multiple homogeneous immune detections based on the FRET process from QDs to GNRs were feasible and conceivable.

In conclusion, the homogeneous immune detection of multiple target antigens is indicated by FRET inducing a quenched fluorescence signal of QDs after constructing the sandwich GNRs–Ab1/Ag/QDs–Ab2 nanostructure. The LOD for HBsAg (or HBeAg) multiple HIA is 9 ng mL$^{-1}$ (or 8.3 ng mL$^{-1}$).

This work was financially supported by National Natural Science Foundation of China (11004188, 60971026, 11074249, and 10904142), the exchange program between CAS of China and KNAW of the Netherlands.

## Notes and references

1 H. Zhang, T. Xu, C. W. Li and M. S. Yang, *Biosens. Bioelectron.*, 2010, **25**, 2402–2407.
2 C. Y. Zhang, H. C. Yeh, M. T. Kuroki and T. H. Wang, *Nat. Mater.*, 2005, **4**, 826–831.
3 G. X. Jiang, A. S. Susha, A. A. Lutich, F. D. Stefani, J. Feldmann and A. L. Rogach, *ACS Nano*, 2009, **3**, 4127–4131.
4 C. Y. Zhang and J. Hu, *Anal. Chem.*, 2010, **82**, 1921–1927.
5 A. M. Dennis and G. Bao, *Nano Lett.*, 2008, **8**, 1439–1445.
6 X. Li, J. Qian, L. Jiang and S. L. He, *Appl. Phys. Lett.*, 2009, **94**, 063111.
7 Q. Zeng, Y. Zhang, X. Liu, L. Tu, Y. Wang, X. Kong and H. Zhang, *Chem. Commun.*, 2010, **46**, 6479–6481.
8 Y. Xia, L. Song and C. Zhu, *Anal. Chem.*, 2011, **83**, 1401–1407.
9 K. T. Yong, W. C. Law, I. Roy, Z. Jing, H. J. Huang and M. T. Swihart, *J. Biophotonics*, 2011, **4**, 9–20.
10 K. T. Yong, I. Roy, H. E. Pudavar, E. J. Bergey, K. M. Tramposch, M. T. Swihart and P. N. Prasad, *Adv. Mater.*, 2008, **20**, 1412–1417.
11 G. X. Liang, H. C. Pan, Y. Li, L. P. Jiang, J. R. Zhang and J. J. Zhu, *Biosens. Bioelectron.*, 2009, **24**, 3693–3697.
12 I. L. Medintz, A. R. Clapp, H. Mattoussi, E. R. Goldman, B. Fisher and J. M. Mauro, *Nat. Mater.*, 2003, **2**, 630–638.
13 C. J. Orendorff and C. J. Murphy, *J. Phys. Chem. B*, 2006, **110**, 3990–3994.
14 E. R. Goldman, E. D. Balighian, H. Mattoussi, M. K. Kuno, J. M. Mauro, P. T. Tran and G. P. Anderson, *J. Am. Chem. Soc.*, 2002, **124**, 6378–6382.
15 Q. Zeng, Y. Zhang, K. Song, X. Kong, M. C. G. Aalders and H. Zhang, *Talanta*, 2009, **80**, 307–312.
16 S. A. Crooker, J. A. Hollingsworth, S. Tretiak and V. I. Klimov, *Phys. Rev. Lett.*, 2002, **89**, 186802.